

McGILL UNIVERSITY

HONOURS THESIS PROJECT

**Pneumatic artificial muscles:
an approach to modelling skeletal
muscles to further understand spinal
stability.**

Author:

Thomas JANSEN

Supervisor:

Prof. Mark DRISCOLL

*A thesis submitted in fulfillment of the requirements
for the Honours Thesis Project (MECH 403)*

in the

Biomechanics Research Group
Department of Mechanical Engineering

April 11, 2019

Declaration of Authorship

I, Thomas JANSEN, declare that this thesis titled, “Pneumatic artificial muscles: an approach to modelling skeletal muscles to further understand spinal stability.” and the work presented in it are my own. I confirm that:

- This work was done in the context of an exchange for two semesters at **McGill University** in Canada, while completing a MEng in Mechanical Engineering at the **University of Bristol** in the United Kingdom.
- Where any part of this thesis has previously been submitted for a degree or any other qualification at this University or any other institution, this has been clearly stated.
- Where I have consulted the published work of others, this is always clearly attributed.
- Where I have quoted from the work of others, the source is always given. With the exception of such quotations, this thesis is entirely my own work.
- I have acknowledged all main sources of help.
- Where the thesis is based on work done by myself jointly with others, I have made clear exactly what was done by others and what I have contributed myself.

Signed:

Date:

MCGILL UNIVERSITY

Abstract

Faculty of Engineering
Department of Mechanical Engineering

MEng in Mechanical Engineering

**Pneumatic artificial muscles:
an approach to modelling skeletal muscles to further understand spinal
stability.**

by Thomas JANSEN

Back pain is believed to be caused by the deterioration of spinal stability and is a pressing issue in terms of global health and productivity. This study explores the use of McKibben style Pneumatic Artificial Muscles (PAMs) as a means to model skeletal muscles, applied in a robotic spine, to further understand the mechanisms behind stability. To do so, a literature review was produced which found that they have similar force-displacement properties but different force-velocity behaviour than biological muscles. However, the relevance of the force-pressure behaviour was unknown. A test bench was therefore designed with purpose to collect force-pressure data. Consequently, the PAMs used in the robotic spine, as well as modified alternatives, were found to exhibit a linear relationship between force and pressure, which correlated with known data from the tibialis anterior of rabbits. Furthermore, by estimating the force in spinal muscles, it was found that the PAMs produced a force of the same order of magnitude. By modifying the outer mesh and inner tube, a wider range of force capabilities was possible. Moreover, variability in results underlined a weakness due to slipping of the fixings from which a concept design was produced. All in all, the PAMs, while presenting certain limitations, proved to be a good starting point for a physical model of skeletal muscles.

Résumé

Muscles pneumatiques artificiels : une approche pour modéliser les muscles squelettiques

Thomas JANSEN

Le mal de dos pourrait tenir son origine dans la détérioration de la stabilité de la colonne vertébrale, et ce tiens d'être un problème urgent en termes de santé, de productivité et de bien-être. Cette étude examine le potentiel des Muscles Pneumatiques Artificiels (PAM) pour la modélisation de muscles squelettiques, appliqués dans un squelette robot, afin d'accroître la connaissance des mécanismes permettant la colonne vertébrale de se stabiliser. A cette fin, une revue des résultats de recherche a été effectué, révélant des propriétés similaires en termes de force/longueur, malgré des différences du comportement force/vitesse, par rapport aux muscles biologiques. Cependant, leurs propriétés force/pression est inconnue. Par conséquent les PAMs furent testé pour obtenir ces dernières. Ceci a permis de montrer que les muscles ressemblent fortement aux muscles biologiques car ils présentent, tous deux, une relation linéaire entre la force produite et la pression.

Acknowledgements

I would like to express my immense gratitude and warmest thanks, first and foremost, to my supervisor, Professor Mark Driscoll for his friendly support and professional guidance. He gave me the opportunity to study in a field that I am passionate about, to be a part of a wonderful research group and gain experience in a purposeful field of work.

My thanks extend to Ibrahim El Bojairami for his unquestioning willingness to help and give advice during the completion of this project. To Emily Newell, for her friendship and support. To Sneha Patel, for welcoming me in the lab with an unwavering smile and a laugh on every occasion. And to all the other members of the **Biomechanics Research Group** that welcomed me with open arms.

I would also like to acknowledge the guidance of Professor Evgeny Timofeev, who helped improve the quality of my work immensely. For which I am grateful for.

Special thanks are due to my partner, Valentine Arnaudo, for her continual support and understanding as she toils away in her medical studies to become a doctor. Our mutual passion for the medical field fueled my efforts and pushed me to produce the best work I could. Finally, I would like to thank my mother and father, without whom I would not be who I am, and where I am today.

Contents

Declaration of Authorship	iii
Abstract	v
Acknowledgements	vii
1 Introduction	1
2 Background	5
2.1 Fundamentals of musculoskeletal biomechanics	5
2.1.1 Spinal stability	6
Defining stability	6
Active and passive stabilization	7
2.1.2 Biomechanics of skeletal muscles	9
2.2 Pneumatic artificial muscles	11
2.2.1 Fundamentals of PAMs	12
2.2.2 Experimentation	13
2.2.3 Analytical modelling	15
3 Methods and results	17
3.1 Methods	17
3.1.1 Experimental setup	17
3.1.2 Data acquisition and treatment	18
3.1.3 Modifications to PAMs	19
3.2 Results	20
3.2.1 Force - pressure curves for the original PAMs	20
3.2.2 Force - pressure curves for the modified PAMs	23
4 Discussion	25
4.1 Performance of the original PAMs	25

4.2	Performance of the modified PAMs	27
4.3	Comparison to biological data	28
4.4	Future work	32
4.4.1	Redesigning the PAMs	32
4.4.2	Improving the Test Bench	33
5	Conclusion	35
	Bibliography	37
A	Data	41
B	Bill of materials	43
C	Muscle force estimation	45

List of Figures

2.1	General force-length (a) and force-velocity (b) curves of biological muscles	10
2.2	Linear relationship between force and pressure in Tibialis Anterior of rabbit from experimental data and FE modelling. <i>TP</i> refers to different cross sections in the FE model. [6, 7, 14]	11
2.3	Diagram of a McKibben style PAM at rest and during activation as a result of air intake.	13
2.4	Typical responses of PAMs during isotonic (concentric) testing (a), and isometric testing (b).	14
3.1	Diagram of the test bench built and used to test the PAMs for this study.	18
3.2	Curve and linear best fit of the force vs. pressure in the original 5" PAM demonstrating an almost linear relationship. The error bars represent the standard deviation which increases with pressure.	21
3.3	Curve and linear best fit of the force vs. pressure in the original 8" PAM demonstrating an almost linear relationship.	22
3.4	Curve and linear best fit of the force vs. pressure in the original 11.5" PAM demonstrating an almost linear relationship.	22
3.5	Curve and linear best fit of the force vs. pressure in the original 11.5" and modified PAMs. Although the linearity remains, the maximum force was increased and decreased by modifying the inner tube and outer mesh respectively.	23
4.1	Linear best fit lines of the data collected from the PAMs used for this study.	29
4.3	Concept fixings for the PAMs. (The outer mesh was not included but would be fixed between the threads and an air inlet should be added at one end)	33

List of Tables

3.1	Summary of the quantifiable properties of all the PAMs tested in this study as well as the results from linear regression.	24
A.1	Data from testing the PAMS	41
B.1	Bill of materials used in the construction of the test bench.	43
B.2	Bill of materials used to modify the original PAMs.	43

List of Abbreviations

CNS	Central Nervous System
CSA	Cross Sectional Area
EZ	Elastic Zone
IMP	Intra-Muscular Pressure
NZ	Neutral Zone
PAM	Pneumatic Artificial Muscle
ROM	Range Of Motion
SFU	Smallest Functional Unit

Chapter 1

Introduction

Back pain is said to be the largest contributor to disability worldwide [1] and according to a 2007 study [2], up to 80% of the population will suffer from back pain at some point in their lives. Unfortunately these figures seem to be on a rising trend, as the years spent with disabilities related to back pain have increased by 54% from 1990 to 2015 [3]. Taking into account an increasingly aging population, the motivation to understand the causes and provide solutions is greater than ever. Moreover, there are many factors that affect the onset of back pain, some less quantifiable than others, ranging from: socioeconomic status, general health condition, physical attributes and psychological state [2]. Although socioeconomic status and psychological state aren't entirely tangible metrics, physical attributes on the other hand, may refer to the nervous structures within the spine. The healthy condition of which can be ensured with effective *spinal stability*, which helps prevent the onset of mechanical deterioration of spinal components [4]. Unfortunately the mechanics of spinal stability are complex and mostly unknown.

That being said, a good understanding of the biomechanics of skeletal muscles and spinal architecture can be used to construct models that help reproduce the

spine's behaviour. Engineers have a wide range of skillsets at their disposal to do so, and several approaches can be employed to study the multiple aspects of the issue. The biggest unknown today relates to the role that skeletal muscles have in the *active* stabilization of the spine. The complexity of modelling spinal stability comes down to the multitude of control surfaces between the muscles and skeletal elements. A complexity which is only exacerbated by the feedback interaction between muscles and the central nervous system (CNS). This is why it is useful to simplify the problem down into its most important features and is the overarching theme of this thesis. It constitutes a small contribution to a greater effort to model spinal stability by several colleagues in the **Biomechanics Research Group** at **McGill University**.

More specifically, it is an attempt at modelling skeletal muscles to understand the role that intra-muscular pressure¹ (IMP) plays in stabilizing the spine. That is to say, how does the pressure built up *inside* the muscles contribute to stabilization? This is a mostly unanswered question due to the difficulty of measuring IMP; currently limited to *in-vivo* devices [5]. Data is sparse because of this and is limited to studies on the tibialis anterior muscle of rabbits [6, 7]. However, there are many approaches to start answering this question and this thesis investigates the possibilities of modelling skeletal muscles with Pneumatic Artificial Muscles (PAMs). These are pneumatic actuators consisting of an expandable tube, wrapped inside a braided mesh and clamped at both ends. As air is introduced, the radial expansion of the inner tube is converted into axial contraction due to the properties of the outer mesh. This effort is part of a bigger project to build a physical model of the spine. This robotic spine was started by Isabella Bozzo, Michael Di Miele, Brandon Malz and Samantha Zielinski for their

¹IMP is defined as the hydrostatic fluid pressure within a muscle

capstone project in 2017. Currently, Laura Fasanella, Benjamin Francolini, Jody Haig and Brittany Stott are implementing control to allow the spine to balance automatically.

The aims of this thesis project however, are to gather data on the current PAMs being used, to describe the relationship between pressure and the resulting contractile force produced by the artificial muscles. By obtaining this data, comparisons can be made between the PAMs and their biological counterpart. Consequently, one can evaluate the validity of using McKibben style muscles as a model for skeletal muscles. Moreover, the performance of the PAMs as actuators should be assessed to predict issues that could surface when applying control to the robotic spine and propose possible improvements to be made.

To start, a literature review of both musculoskeletal biomechanics and pneumatic artificial muscles is presented in Chapter 2, to provide a thorough understanding of the multiple facets of this project. Consequently, the methods used and ensuing results are presented in Chapter 3. This mostly includes the design and build of the test bench, the experimental procedure, modifications made to the PAMs and the resulting force-pressure curves. Chapter 4 then discusses these results by exploring various aspects: the performance of the original and modified PAMs as actuators, a comparison to biological muscles and a concept design to improve the PAMs. Finally, Chapter 5 serves as a conclusion to the project.

Chapter 2

Background

To be able to fully understand the scope of this project it is important to first lay the ground work and cement key aspects regarding the biomechanics of the spine, biological and pneumatic artificial muscles. To this end, two literature reviews are necessary. A first review provides an introduction of spinal stability and biological muscle mechanics, in the hopes to convey the difficulty of tackling such an issue; who's very definition is still debated. Following this, a second review hopes to provide the reader with a solid understanding of pneumatic artificial muscles ranging from historical considerations, to various analytical models, methods of experimentation and real world applications.

2.1 Fundamentals of musculoskeletal biomechanics

The spine is a complex system composed of numerous parts which all work together to provide the upright position that we very much enjoy as bipedal apes. It is controlled by muscles which support the head and trunk during posture and movements whose behaviour is controlled by the central nervous system

(CNS). This section will be looking at how these muscles work and how they relate to spinal stability.

2.1.1 Spinal stability

Defining stability

As previously mentioned, spinal stability is the fundamental requirement to protect the nervous structures of the spine which can help prevent the early mechanical deterioration of spinal components [4]¹. But what is spinal stability? How does one define it and what are the key factors at play?

As it turns out, a consensus definition is yet to be reached, but one can start by defining *instability*, which is usually considered as the increase in movements which lead to back pain. Conversely, *stability* can be defined as the capacity of the spine to remain cohesive and preserve reasonable displacements. The latter referring to displacements which do not cause damage to the spinal cord and nerve roots. This description paraphrases definitions proposed by White et al. and the American Academy of Orthopedic Surgeons [8] [9]. One might start to wonder what is preventing displacements in the first place and this comes down to the various components of the spine. The smallest unit of which is the vertebra, also referred to as the smallest functional unit (SFU) of the spine [4]. A combination of main and coupled motion can be achieved by the vertebra but these are limited by bony and soft restraints. It is when these restraints lose integrity that spinal stability is affected.

¹Please note that section 2.1.1 is heavily inspired by R. Izzo et al.'s review of spinal stability [4]

A useful analogy was proposed by Panjabi to understand the load-displacement characteristics of the spine. One can visualize an unstable spine as a small ball in a large bowl. In this scenario, it doesn't take much force/tilt to make the ball move: it is unstable. In comparison, the analogy of a stable spine is that of the same ball in a wine glass. It takes a lot more tilting to make the ball move up the walls of the glass [10]. This introduces two concepts related to the physiological range of motion (ROM): the neutral zone (NZ) and the elastic zone (EZ). The NZ is where the spine can move with low resistance. It is followed by the EZ where resistance to movement is higher, requiring more load per unit displacement [4]. In the analogy, the NZ is the base and the EZ are the walls of the recipient. The larger the NZ, the more severe the instability will be. This explains why spinal fusion is used to alleviate the symptoms of debilitating back pain. This procedure limits the ROM and reduces the NZ of the spine and frees the patient from back pain. As one could gather, it is hard to define what spinal stability is exactly, even harder to measure clinically.

Active and passive stabilization

Having a general idea of what spinal stability refers to, it is now of interest to identify the mechanisms which provide stabilization. These can be split into two categories: active and passive stabilization. In fact, an alternative definition of spinal stability was also proposed by Panjabi, as the inability of these mechanisms to maintain the spine within physiological limits of the NZ of the vertebra [11].

Indeed, the spine stabilizes itself as a consequence of the effective interactions between three disparate systems [4]. These are:

- the spinal column (the passive subsystem),
- the muscles (the active subsystem),
- and the central nervous system which acts as the control unit.

Passive stabilization refers to the structural components of the spine: the bones, disks and ligaments. These govern the EZ and provide rigidity to prevent the whole system from collapsing. It relies on the healthy functioning of the vertebral architecture, bone density, inter-vertebral disc joints, facet joints, ligaments and physiological curves. The details of which are relatively well understood and explained in more detail in R. Izzo et al.'s 2013 review article [4]. However, this level of understanding is sufficient information for the purposes of this review.

Active stabilization on the other hand refers to the muscles and tendons which intuitively provide stability in the NZ where resistance to movement is low [4]. However, the complexity of how all these relate together prohibits a good understanding of active stabilization. This is due to the multitude of muscles involved, and their complex antagonistic relationships. Furthermore, the configuration and multiplicity of control surfaces (spinal insertion sites and fascia) makes it incredibly difficult to obtain a cohesive understanding of this interconnected system [4].

This cements the importance of the work being done in the **Biomechanics Research Group** and underlines the overarching objective of this project: to develop a better understanding of spinal stability. As previously mentioned, for serious cases of chronic back pain, the current surgical procedure is spinal fusion which hinders mobility. However, with a better understanding of the dynamical

influences at play, one could design better solutions that are adapted to the way the spine actively stabilizes itself.

2.1.2 Biomechanics of skeletal muscles

Having an understanding of the bigger picture of this project, it is now time to dig deeper into the behaviour of skeletal muscles, to allow for informed discussion to be had regarding the validity of the PAMs being used in the robotic spine, as models for skeletal muscles.

Skeletal muscles attach to the skeleton through tendons and fascia and can only provide a pulling force. Consequently, every motion of the body needs an antagonistic pair which pull in opposition to work effectively. This allows the skeleton to actuate its multitude of degrees of freedom as well as provide protection during movement. The pulling action is triggered by neural signals which cause strands in the muscle to slide along each other, converting chemical potential energy to mechanical energy [12]. There is a distinction between concentric and eccentric contraction. The former describes a shortening muscle where as the latter denotes a lengthening muscle. These are isotonic contractions as opposed to isometric contractions, during which the length is constant.

The *force-length* and *force-velocity* properties of biological muscles are relatively well known. Models such as the Hills Muscle Model have been validated through experimentation [13] and serve as a tool to predict muscle behaviour. In summary, the *active* force produced is maximal at resting length and decreases as the muscle is extended or contracted. This is due to the interaction of the aforementioned strands within the muscle which become detached during excessive extension and can't slide further during excessive contraction. However, the

passive force allows the overall tension to support higher loads during excessive extension [12]. A typical *force-length* curve for biological muscles is shown in Figure 2.1a.

The velocity of the contraction also has an impact on the resultant force. During shortening (concentric contraction), the higher the velocity, the lower the resultant force will be. Conversely, the force increases with velocity during lengthening (eccentric contraction) but quickly reaches a plateau [12]. The typical *force-velocity* response of muscles is shown in Figure 2.1b.

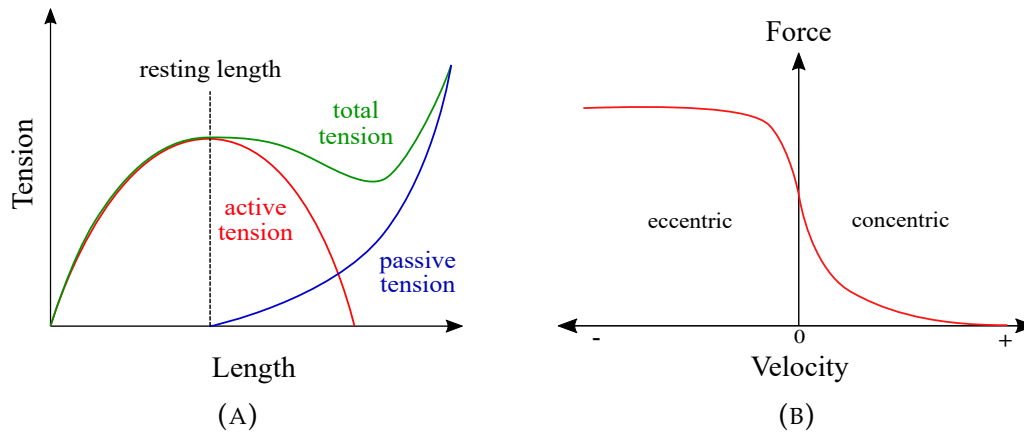


FIGURE 2.1: General force-length (a) and force-velocity (b) curves of biological muscles

On the other hand, the *force-pressure* properties of biological muscles are unknown for the most part and studies have been limited to the *tibialis anterior* muscle in rabbits [6, 7]. However, Ibrahim El Bojairami, a PhD candidate in the **Biomechanics Research Group at McGill University**, has used this data to validate a finite element model of the muscle [14]. The result of which is shown in Figure 2.2 and shows a linear relationship between force and pressure. The linearity would suggest an ability to extrapolate the results to the general function of biological muscles but this is unconfirmed.

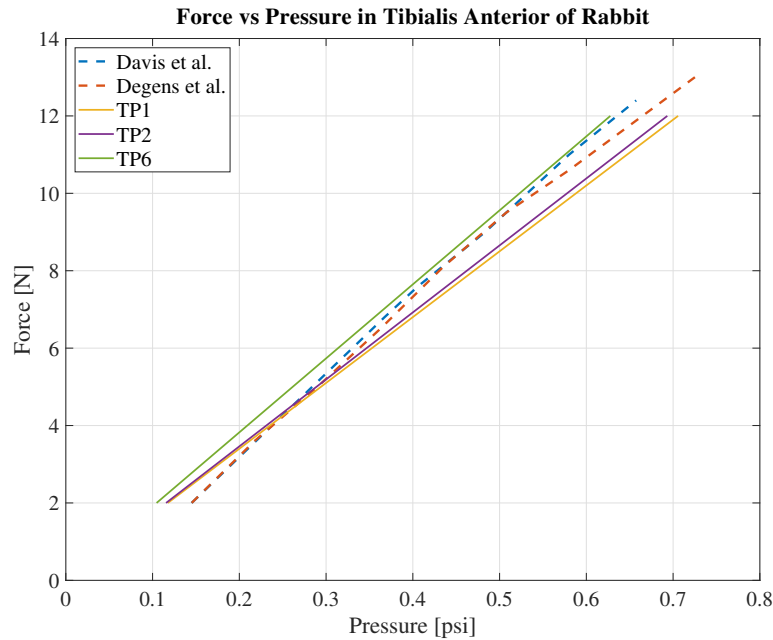


FIGURE 2.2: Linear relationship between force and pressure in Tibialis Anterior of rabbit from experimental data and FE modelling. *TP* refers to different cross sections in the FE model. [6, 7, 14]

2.2 Pneumatic artificial muscles

There are different approaches to modelling muscles to start understanding spinal stability. An in depth approach is to develop a Finite-Element model. This has the advantage of being accurate if reasonable assumptions are used, but can be very complex to implement for reasons outlined in section 2.1. In fact, Ibrahim El Bojairami is currently developing a model of the spine for this purpose. Alternatively, physical analog models can be useful to develop an intuition for how the mechanisms operate. This is why Pneumatic Artificial Muscles (PAMs) are being investigated: to determine to what extent these constitute a valid approach to modelling biological muscles. In the robotic spine there are three different PAMs, of varying lengths, attempting to model the *psoas major* (8" PAM), the *erector spinae* (8" and 5" PAM) and the *rectus abdominus* (11.5" PAM).

2.2.1 Fundamentals of PAMs

In fact, PAMs have been studied for their operational similarity to biological muscles. However, soft pneumatic actuators come in various forms:

- Planar membranes or inflatable compression sleeves for therapeutic purposes [15],
- in Bellows configuration [16],
- and cylindrical McKibben style actuators.

The last of which being the focus of this report. Indeed, PAMs is a broad term encompassing actuators that use air or liquid interacting with a soft material to provide pressure or force. In his 2012 review, B. Tondu described artificial muscles as being *“founded on a general ‘equilibrium principle’ according to which the the artificial muscle in response to constant stimulus, changes its shape from a given equilibrium position to another one”* [17]. McKibben style PAMs in particular, have garnered a lot of attention in research and industry. This is thanks notably to their vibration absorbing properties useful in industrial machining, most notably utilized by FESTO [18]. They are also used in soft robotics for their ability to mimic the behaviour of their biological counterparts. Examples of which are FESTO’s *Airic Arm* [19], a 7-DOF manipulator developed by Tondu et al. [20], and a bipedal robot developed by B. Verrelst et al. [21].

Similarly to muscles they can only apply force in one direction and require an antagonistic pair to work effectively. They are made up of an inner expandable tubing, wrapped inside a braided mesh and clamped at both ends. Air is introduced at one end which makes the inner tube expand and, due to the properties

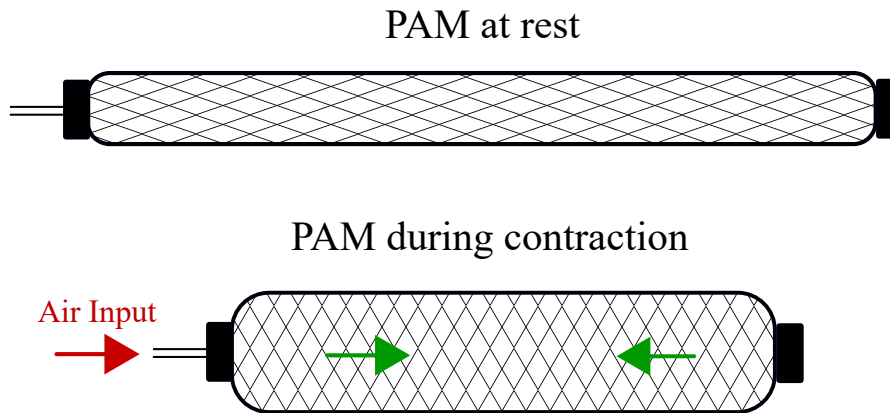


FIGURE 2.3: Diagram of a McKibben style PAM at rest and during activation as a result of air intake.

of the braided mesh, an axial contraction occurs. Thanks to the weaving of filaments which compose the braided mesh, the radial expansion of the inner tube makes these filaments slide over each other, converting the expansion to axial contraction. In fact, the available contraction ratio, a measure of length reduction, and the contractile force of a PAM are functions of its initial braid angle [17]. A simplified diagram of these types of PAMs is shown in Figure 2.3.

2.2.2 Experimentation

Similarly to biological muscles there are various tests one can perform to characterize the performance of PAMs. Most notably: isometric (constant length) and isotonic (varying length) tests.

Isometric tests can be run by clamping the muscle at both ends, restricting its movement. One clamp should have a load cell to measure the force as the pressure is being introduced and measured by a pressure gauge. Both quasistatic and dynamic tests can be run. The former involves inputting the air slowly to

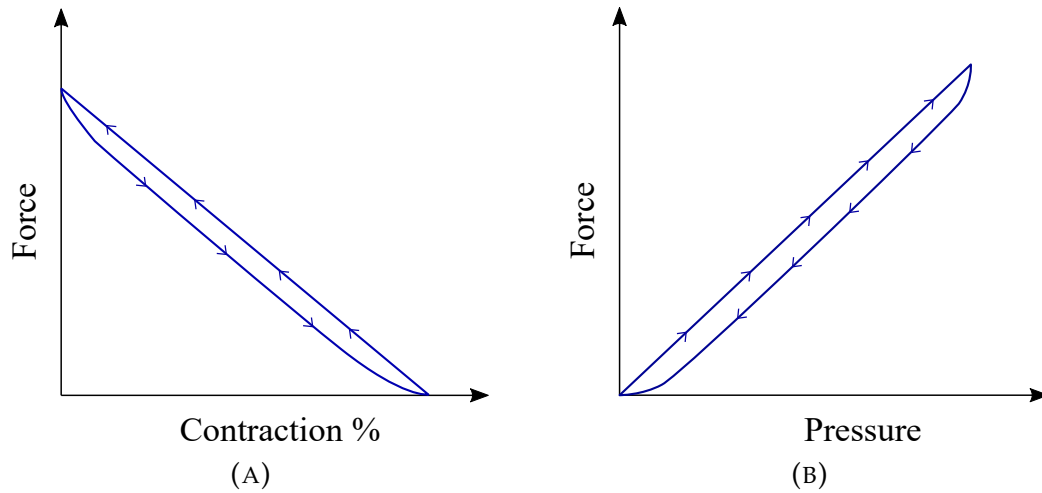


FIGURE 2.4: Typical responses of PAMs during isotonic (concentric) testing (a), and isometric testing (b).

yield a *force-pressure* curve whereas the latter involves rapidly opening the valve which yields a *force-time* curve indicative of the response rate. *Force-pressure* curves for McKibben PAMs are relatively linear depending on the hysteresis caused by the friction within the braided mesh and between the mesh and the inner tube. A typical *Force-pressure* response is shown in Figure 2.4b.

Isotonic tests² on the other hand have a similar setup, except that the muscle is free to move at one end. Pressure is held at a constant value till the muscle reaches equilibrium and is then released. This type of testing yields a *force-displacement* curve and usually involves testing the displacement with various constant loads attached to the free end. A typical *force-displacement* response is shown in Figure 2.4a.

However, the most common modes of experimentation in the literature are either *force-length* or *force-velocity* experiments. This is because they are easily compared to biological muscle data or the Hill's muscle model for validation. As

²these are isobaric tests and are analogous to concentric contraction in biological muscles

previously stated, *force-pressure* curves are hard to obtain on biological muscles which makes it hard to validate these types of curves obtained from PAMs. In Chou and Hannaford's 1996 study, it was found that although the actuators' *force-length* properties are similar to biological muscles, their *force-velocity* properties are not [22]. They proposed the addition of parallel and serial elastic and viscous elements to improve static and dynamic performance. Consequently a study by Klute, Czerniecki and Hannaford found similar results and followed up on the proposal by designing a parallel damper to ameliorate the *force-velocity* performance of the PAMs [23]. This was done by modelling an ideal Hill-like damper which only modestly improved the shape of the curve to further match a biological muscle 'envelope'.

Unfortunately a parallel damper would be very hard to implement in the context of the robotic spine due to complexity of the actuator/skeleton attachments and the need for "soft" elements which should comply with the skeleton's motion. The *force-length* properties during isotonic contraction of the PAMs being used in this project were logged during I. Bozzo et al's Capstone project in 2017. Disregarding the possibility of improving the *force-velocity* performance of the PAMs this leaves the question of their *force-pressure* properties. The obtaining of which is the objective of this project. Not only to be able to provide the data to help B. Stott et al's capstone project but to discuss the similarities and differences with biological muscles.

2.2.3 Analytical modelling

Mathematical and physical modelling is useful to the extent that it provides a fast and cost effective way to predict how differences in a PAM's variables affect

its performance. Early attempts included static models relating force to pressure in a linear function of the braiding angle [22]. However, this assumed zero thickness and ignored vena contracta effects at the end fixtures. Other models were developed which relied less heavily on assumptions but required experimentally derived constants [24]. More recently however, a model was derived to include end fixture effects without the need of experimental constants, making it the most applicable to a wide range of scenarios [25]. Several conclusions on the behaviour of PAMs can be made by using these models which provide useful insight to modify their performance. These are listed below:

- The lower the initial braid angle α_0 , the higher the force F and the contraction ratio $c\%$ will be. [17].
- Theoretical max braiding angle is 54° , which limits the range of α and therefore the contraction ratio. Another motivation to have the lowest initial braid angle to increase range of motion[17].
- Static force (isotonic testing) is most sensitive to the initial braid angle α_0 , less sensitive to initial radius r_0 and almost independent of initial length l_0 [24].
- The length to diameter ratio should be at least 14 to minimize tip effects [23].
- Hysteresis caused by friction effects causes a differentiation between contraction and elongation [17].

These guidelines were particular useful to inform the choice of new components. In the context of the *Robotic Spine Project*, obtaining a wider range of force capabilities is useful to mimic the different types of muscles that are being modelled.

Chapter 3

Methods and results

The following chapter details the methods used to acquire data from the PAMs and the results from the ensuing experiments. Section 3.1 details the design of the test bench required to obtain the *force-pressure* properties of the PAMs used in the *Robotic Spine Project*, the data acquisition and treatment methods as well as the choice of new components to modify their performance. The results are documented and described in Section 3.2.

3.1 Methods

3.1.1 Experimental setup

The *force-pressure* properties of the PAMs were obtained using a test bench designed with the specific objectives in mind. A 2x4 plank of wood was used as a base in which the fixings were placed. These consisted of eye-bolts that screwed into the wood, serving as anchor points to which the actuator and digital force-gauge attached. One eye-bolt was placed at one end of the plank for the force

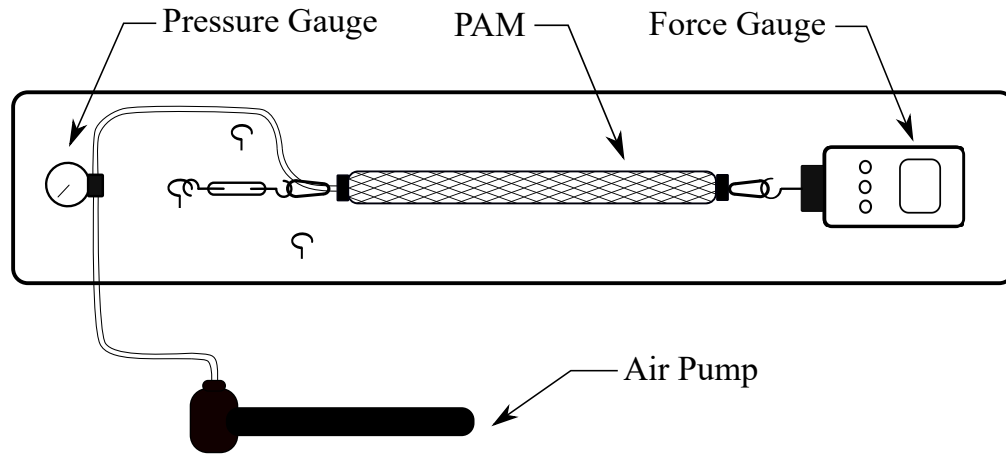


FIGURE 3.1: Diagram of the test bench built and used to test the PAMs for this study.

gauge and three others were set at specific distances matching the length required for the three different PAMs. Connections at each end of the muscles were made using quick-release carabiners and a small turnbuckle at one end to adjust the tension. Moreover, an analog pressure gauge was also fixed to the base through which air was supplied by a hand bike pump, ultimately connecting to the PAM. A diagram of the test bench is shown in Figure 3.1 and the bill of materials is documented in Table B.1 in Appendix B.

3.1.2 Data acquisition and treatment

The muscle was pre-tensioned before air was supplied, after which the pressure and force were read from the pressure-gauge and force-gauge respectively. The analog pressure-gauge, acquired from McMaster, had a range of 0 to 100 psi with 2 psi increments. The digital force-gauge, acquired from Amazon, had a range of 0 to 3000 N with increments of 1 N. The force was recorded every 4 psi

using Microsoft Excel and a total of 5 independent tests were run for each PAM, after which the results were averaged to yield a final response. To account for experimental error the standard deviation was calculated across the 5 tests at each data point using the *stdev.s* function in Excel. This was then used as error bars on the *force-pressure* graphs plotted using Matlab. A linear best fit line was also determined using the "Linear Trendline" function in Excel.

3.1.3 Modifications to PAMs

To study the variability in performance of the PAMs, modifications were made where possible. Notably, the inner tube was changed from the original Silicone Rubber tubing with a hardness rating of 50A Durometer, to a "Super-Soft" Latex tubing with hardness rating of 40A Durometer. Moreover, the braided mesh was changed from the basic expandable sleeving to an Abrasion-Resistant alternative. Although the inner tubing and outer mesh were modified, the radius and length of the muscle was held constant. Finally, data was acquired from the two new PAMs: one with the new inner tubing and original parts and the other with the new outer mesh and original parts. These were made at a length of 11.5" in order to be compared to the original 11.5" PAM. The reasoning behind the selection of these components is detailed in Section 4.2 and the bill of materials is documented in Table B.2 in Appendix B.

3.2 Results

The *force-pressure* curves of the original PAMs used in the *Robotic Spine Project* are shown in Figures 3.2, 3.3 and 3.4. The results for the modified PAMs are shown in Figure 3.5. Further details including the *maximum force*, *widest standard deviation*, the *average of the difference between force in and out*, the *linear best fit function* as well as the R^2 value are tabulated in Table 3.1.

3.2.1 Force - pressure curves for the original PAMs

A linear relationship between pressure and the resultant force can be observed in all three cases. The maximum force produced increases with length by 9% and 25% for the 8" and 11.5" respectively compared to the 5" PAM. For the 5", 8" and 11.5" PAMs, the maximum forces are 205 N, 224 N and 256 N respectively and are produced at the maximum pressure of 90 psi.

The static force during contraction (ie: when the air being pumped into the muscle) is larger than that of the force during extension (when the air is released). This behaviour was quantified by taking the difference in force at each data point and averaging the results (see $\bar{\Delta F}$ in Table 3.1). This property varies from muscle to muscle but only by a minimal amount for the original PAMs.

Furthermore, there is a delay in the force response at low pressures. That is to say, a force is only produced after a pressure threshold is reached after which the force increases linearly. This behaviour is exaggerated during extension, during which the force reaches a null value at a higher pressure than during contraction.

Moreover, the standard deviation represented by the error bars in Figures 3.2,

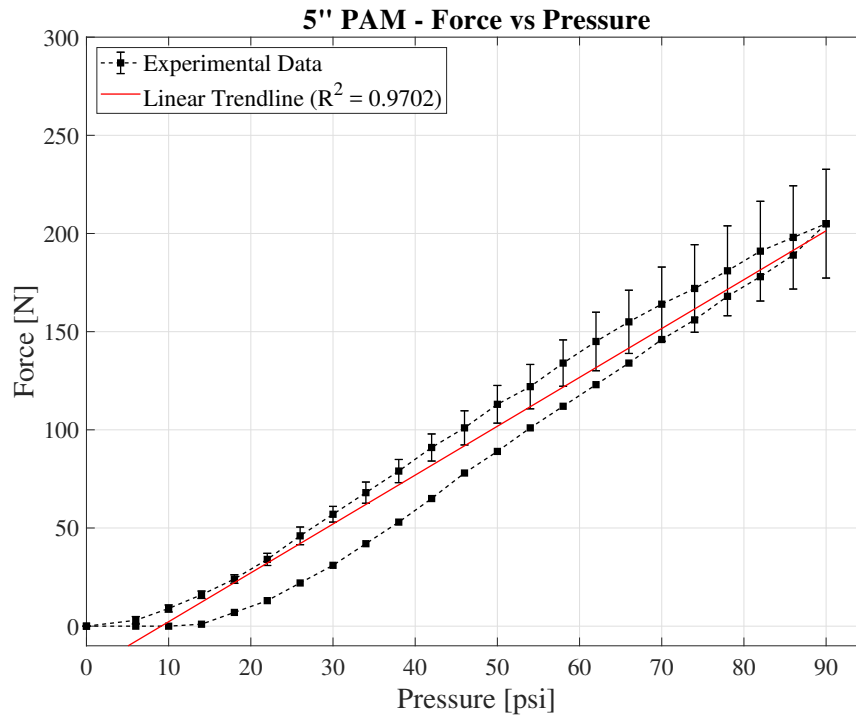


FIGURE 3.2: Curve and linear best fit of the force vs. pressure in the original 5" PAM demonstrating an almost linear relationship. The error bars represent the standard deviation which increases with pressure.

3.3 and 3.4 become larger with increasing pressure. The widest standard deviation in the data is consistently found at the maximum pressure of 90 psi and is tabulated in Table 3.1. The reader should note that the error bars during elongation were omitted for clarity but exhibited a different behaviour: the width of the standard deviation remained relatively constant as the pressure decreased.

Finally, lines of best fit were produced to fit all data points including both the forces during contraction and elongation. The resulting functions are tabulated in Table 3.1 along with their R^2 value.

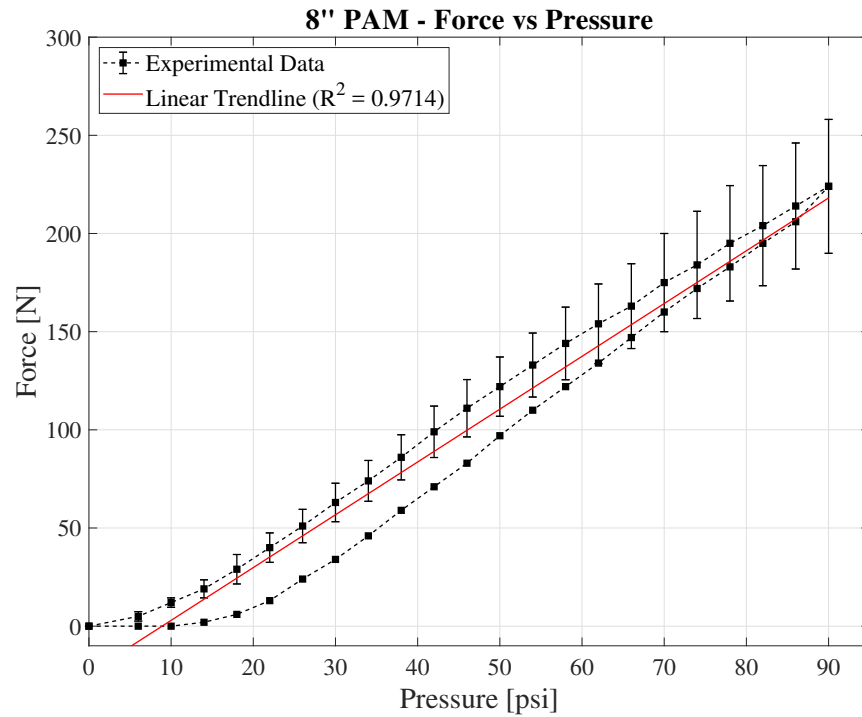


FIGURE 3.3: Curve and linear best fit of the force vs. pressure in the original 8" PAM demonstrating an almost linear relationship.

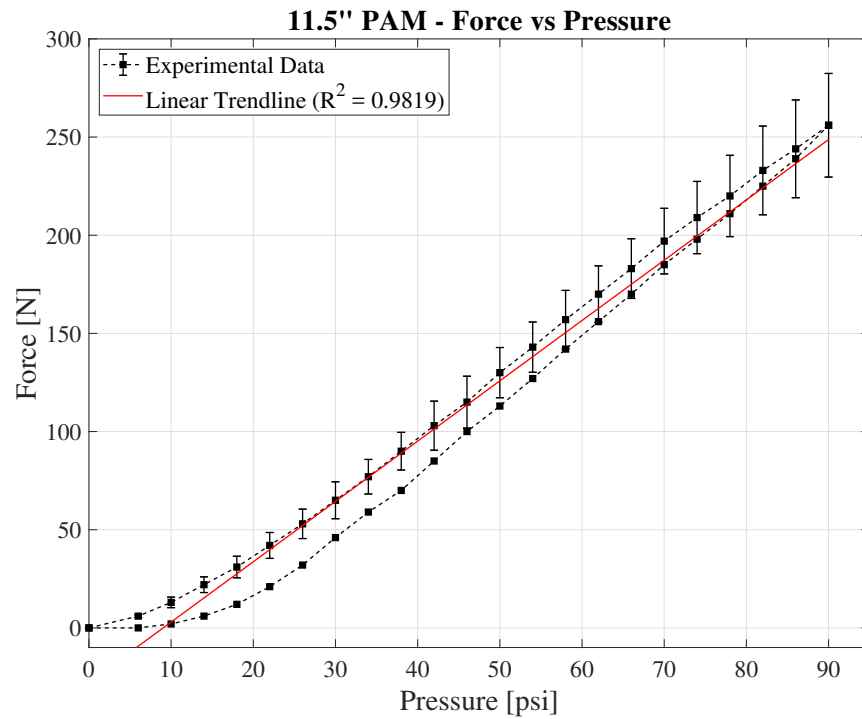


FIGURE 3.4: Curve and linear best fit of the force vs. pressure in the original 11.5" PAM demonstrating an almost linear relationship.

3.2.2 Force - pressure curves for the modified PAMs

The same linear behaviour is found in the modified PAMs (Figure 3.5). However, modifying the inner tube to a softer material produced a 14% increase in the maximum force produced (292 N) and an increase in ΔF by 54% (20 N). Conversely, modifying the outer mesh to an abrasion resistance material resulted in a 54% decrease in the maximum force (164 N) and a 38% decrease in ΔF (8 N). Finally, the other parameters behaved in very much the same way as the original PAMs.

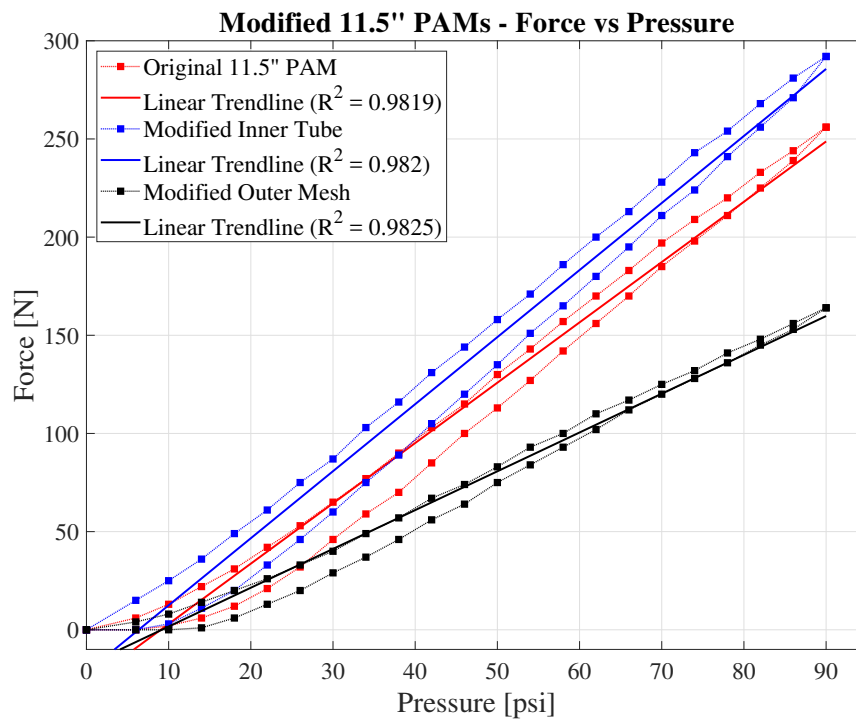


FIGURE 3.5: Curve and linear best fit of the force vs. pressure in the original 11.5" and modified PAMs. Although the linearity remains, the maximum force was increased and decreased by modifying the inner tube and outer mesh respectively.

TABLE 3.1: Summary of the quantifiable properties of all the PAMs tested in this study as well as the results from linear regression.

PAM	Max Force [N]	Widest Std. Deviation [N]	ΔF [N]	Linear Best Fit	R ²
5"	205	27.7	17	$y = 2.4889x - 22.63$	0.9702
8"	224	36.3	18	$y = 2.6895x - 23.949$	0.9714
11.5"	256	26.4	13	$y = 3.0719x - 27.748$	0.9819
Inner Tube Mod.	292	25.8	20	$y = 3.4148x - 21.669$	0.982
Outer Mesh Mod.	164	19.1	8	$y = 1.9768x - 18.119$	0.9825

Chapter 4

Discussion

The ensuing discussion expands on the different properties of the PAMs shown in Chapter 3, why they occur and what impact they have on the performance of the robotic spine. The performance of the original and modified PAMs are considered in Section 4.1 and 4.2 respectively. Moreover, a comparison with their biological counterpart is made in Section 4.3. Finally, Section 4.4 proposes future improvements to be made to the PAMs and work-bench.

4.1 Performance of the original PAMs

Unlike the predictions made in the model proposed by Tondu in 2000, the muscles used in the robotic spine do have some length dependence. However it is only minimal which could be a limitation when trying to model different muscles as one may need to obtain a wider range of force capabilities than is possible with the original PAMs. Not knowing what the force output of the *psaos major*, *erector spinae* and *rectus abdominus* are, it is hard to tell exactly. The force amplitude would most probably not be the same but the ratio of forces between the

PAMs might, or could be adjusted accordingly. This is why a study of the impacts of modifying elements of the PAMs is useful (see Section 4.2) and where a scaling factor can be helpful to scale the loading applied to the spine, adjusted to the capabilities of the PAMs (see Section 4.3).

The standard deviation was shown to increase with force. This is because of slipping at the fixings which cause a variability in the results at higher forces. Indeed, the connections at the ends simply consist of the mesh being looped and tied with zip ties. A rigid connector would mostly solve this problem (a concept design is proposed in Section 4.4). This property is important to keep in mind while applying control to the robotic spine as reliability may become an issue. Another observation linked to the sliding was that the maximum force recorded during the first test was small relative to the following runs, contributing to a large standard deviation, whose value asymptotes despite making multiple tests. This was in part due to the elongation of the muscle with each iteration of testing, which could cause issues in the robotic spine if tension adjusters are added. This also highlighted an issue with the test bench, which could benefit from a length adjusting feature more significant than a turnbuckle (see Section 4.4).

Moreover, the hysteresis in the muscles, quantified by ΔF in Table 3.1, is problematic from a control point of view as the PAMs lack the predictability required for precise actuation. A way to tackle this issue would be to obtain two equations describing both the contraction and elongation modes of the PAMs and use each depending if air is being introduced or released. However, one equation was used to fit the data for simplicity. The variability of ΔF is minimal between the original PAMs with the exception of the 11.5" PAM, most probably due to measurement noise as the material is unchanged.

4.2 Performance of the modified PAMs

A wider range of maximum forces was obtained by making modifications to the inner tubing and outer mesh. As mentioned previously, this is particularly useful to model variability in biological muscles. It should be noted however, that although the materials were changed, the dimensions were not. This is because changing the initial radius, r_0 , would have required redesigning the whole PAM from scratch which was beyond the scope of the project. Moreover, the initial braiding angle, α_0 , is hard to measure and therefore assembling the PAM at a specific initial angle is even more challenging. Nevertheless, the modifications which were relatively easy to implement provided useful insight.

The higher force in the modified inner tube PAM is related to the reduced hardness of the selected tubing. As a consequence of the modification, there was less resistance to a given pressure which yielded higher forces. Conversely, one can conclude that if lower forces were required, a harder material should be chosen (readily available from McMaster Carr). Another observation is that the hysteresis was greater for this PAM than the original which can be due to experimental noise or the interaction between the latex (as opposed to nylon) and the braided mesh.

Moreover, modifying the outer mesh yielded a lower force and lower hysteresis. The latter can be explained by the abrasion resistance of the material, making it easier for the strands to slide over each other, while the former could be due to the thicker strands which provided a greater resistance to expansion. Although the mesh lowered the maximum force it also prevented slipping at the fixings which translated to a narrower standard deviation. This has important implications on the reliability one can expect from these PAMs. Indeed, the new outer

mesh could be used to improve the reliability of the robotic spine if the forces are large enough (although it is only a matter of scaling so this shouldn't be a problem). However, unlike the hardness of the inner tubing, the properties of the outer mesh are harder to quantify and alternatives are limited on McMaster Carr. Therefore, it is hard to translate the insight obtained from this testing to predict how other braided meshes would behave.

In short, the resultant force can be readily modified by choosing an inner tube of varying hardness, while the reliability can be improved by using an abrasion resistant outer mesh.

4.3 Comparison to biological data

The performance of the PAMs as *actuators* in the *robotic spine* were outlined in Sections 4.1 and 4.2. But how do they compare to biological muscles?

As outlined in Chapter 2, the *force-pressure* behaviour of muscles, in general, is mostly unknown. However, a linear behaviour was found to characterize the relationship between force and pressure in the tibialis anterior of rabbits [6, 7, 14]. The results of these studies are shown again in Figure 4.2 to ease comparison with the behaviour of the PAMs shown in Figure 4.1. The latter plots the linear best fit functions, found in Chapter 3, of all the PAMs tested in this study.

What is immediately noticeable is the striking linearity of both the biological and artificial muscles. These are promising results in favor of PAMs as a model for biological muscles, although some variability should be taken into account. Notably, the magnitude of the the forces and pressures.

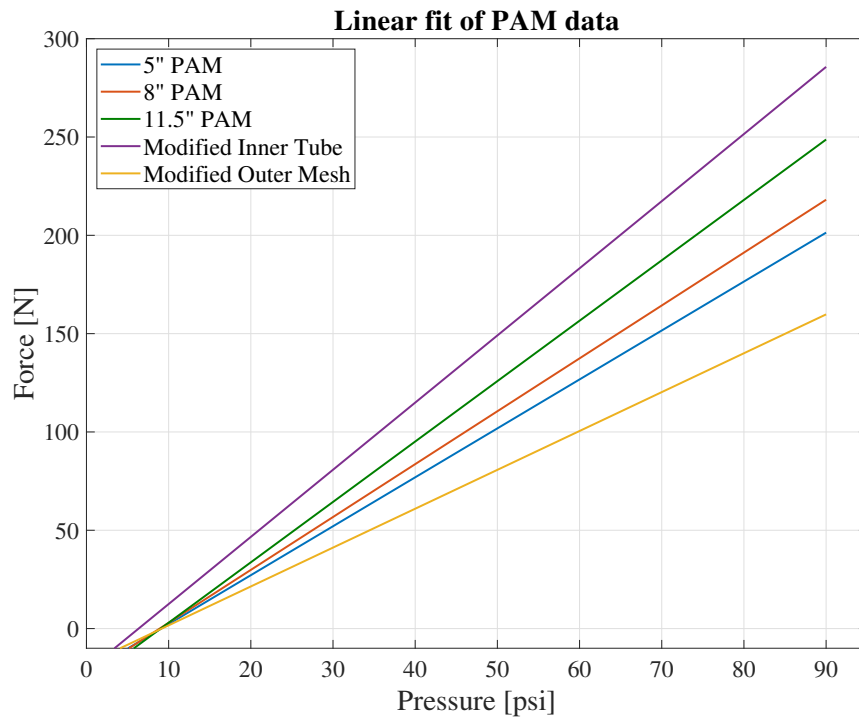


FIGURE 4.1: Linear best fit lines of the data collected from the PAMs used for this study.

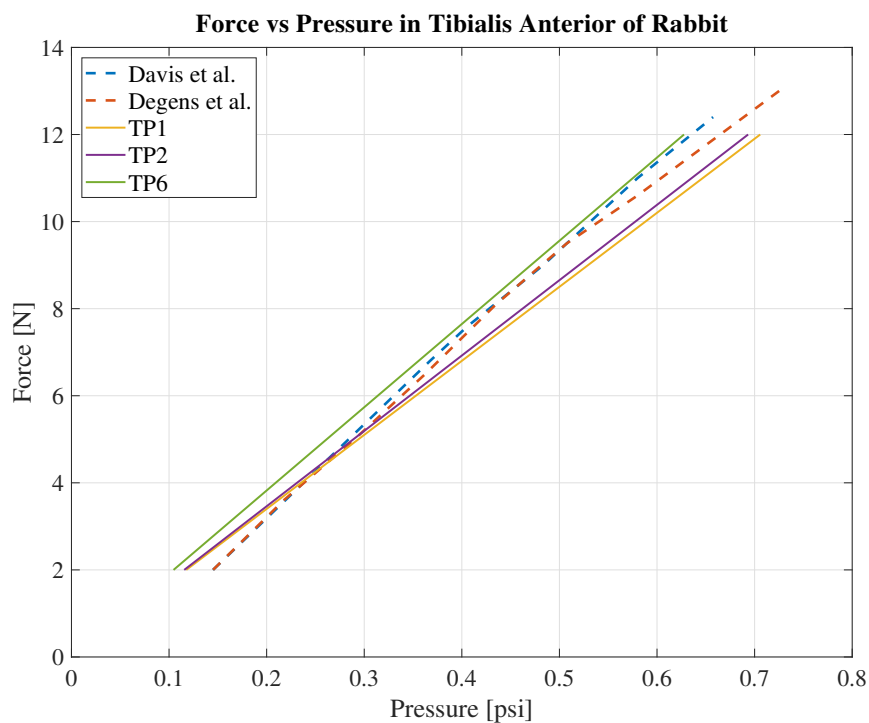


FIGURE 4.2: Linear relationship between force and pressure in Tibialis Anterior of rabbit from experimental data and FE modelling. *TP* refers to different cross sections in the FE model. [6, 7, 14]

A range of 160 to 300 N maximum force is produced by the PAMs where as the *tibialis anterior* only produces 12 N maximum. Moreover, the order of magnitude of pressure is about 100 psi in the PAMs compared to 0.1 psi in the biological muscles. This can come down to the differences between biological processes and purely mechanical actuation. That being said, size may be playing an important role here. The *tibialis anterior* of the rabbit is very small compared to the muscles the PAMs are attempting to model: *psoas major*, *erector spinae* and the *rectus abdominus*.

Indeed, the volume of the *tibialis anterior* is only about 3.4 cm^3 (with a cross sectional area of 0.6 cm^2), compared to the *psoas*' volume of 155 cm^3 [26, 27]. Therefore, one would expect the forces in the spinal muscles to be much higher than those of the *tibialis anterior*. Consequently, an estimate of the force in the *multifidus*¹ muscle was made to make an informed comparison between the biological muscles in the spine and the PAMs. This consisted in using the linearity to scale the slope of the *tibialis anterior* with a scaling factor based on cross-section². It was found that the muscle produced about 750 N of force at a pressure of 200 mmHg (3.9 psi). The derivation can be found in Appendix C.

The important take away is that the forces produced by the PAMs and a spinal muscle are of the same order of magnitude. Since measurements of force output by spinal muscles aren't readily available, one can only conclude this way. Ultimately, in the context of the *robotic spine* project, the objective would be to scale the forces being applied to the model, keeping in mind the capabilities of the PAMs, so as to apply realistic loading conditions.

¹chosen as a point of comparison based on available data

²volume could also be used

Moreover, there are assumptions and limitations to keep in mind regarding the PAMs as a model for spinal muscles:

- No implementation of tendon or fascia - only direct rigid attachments to bones. Lacks the interconnected nature of spinal elements outlined in Section 2.1.
- The ratio of radial expansion and axial contraction is much less in PAMs than in biological muscles, which would make it hard to study the *inter-muscular*³ pressure. This would be particularly interesting to do as it is believed that the muscle to muscle interaction plays a key role in stabilizing the spine.
- Only certain muscle groups have been modelled for simplicity.
- The force-velocity behaviour will be very different than biological muscles.

Despite these limitations, this paper believes that the PAMs are a good start to modelling spinal muscles in the context of the *robotic spine* project. Although it constitutes a fairly simplified model of how the spine behaves, it can provide useful insight and help develop an intuitive understanding of which muscle groups are used in different scenarios. Taking into account the literature review in Chapter 2, one can conclude that although the *force-velocity* properties aren't accurate, the *force-displacement* and *force-pressure* behaviour have similarities with biological muscles.

³Interaction between muscles which is different from intra-muscular pressure which is the pressure in the muscle

4.4 Future work

Having discussed the performance of the PAMs, Section 4.4.1 and 4.4.2 propose future work to improve the practical aspects of the PAMs and test bench. These are based on issues that arose during testing mostly due to slipping at the fixings.

4.4.1 Redesigning the PAMs

Other than changing the material, the configuration could be changed to improve the ease with which the PAMs are assembled as well as the consistency in performance. By nature of using zip ties to fix the components, the assembly process is highly variable and depends on the method and person operating. Moreover, this was a source of slipping which caused variability during testing. To address these issues the concept, shown in Figure 4.3, was designed. The fixing consist of two elements. One with a female thread and rigid connector, the other with a male thread and friction fit to accommodate the tubing. Once the tubing is placed on to the latter part, the mesh should placed in such a way that it is wedged between the two parts as they are screwed on together. An air inlet should be present in one of the ends. This concept should solve the aforementioned issues but has the disadvantage of having to be manufactured.

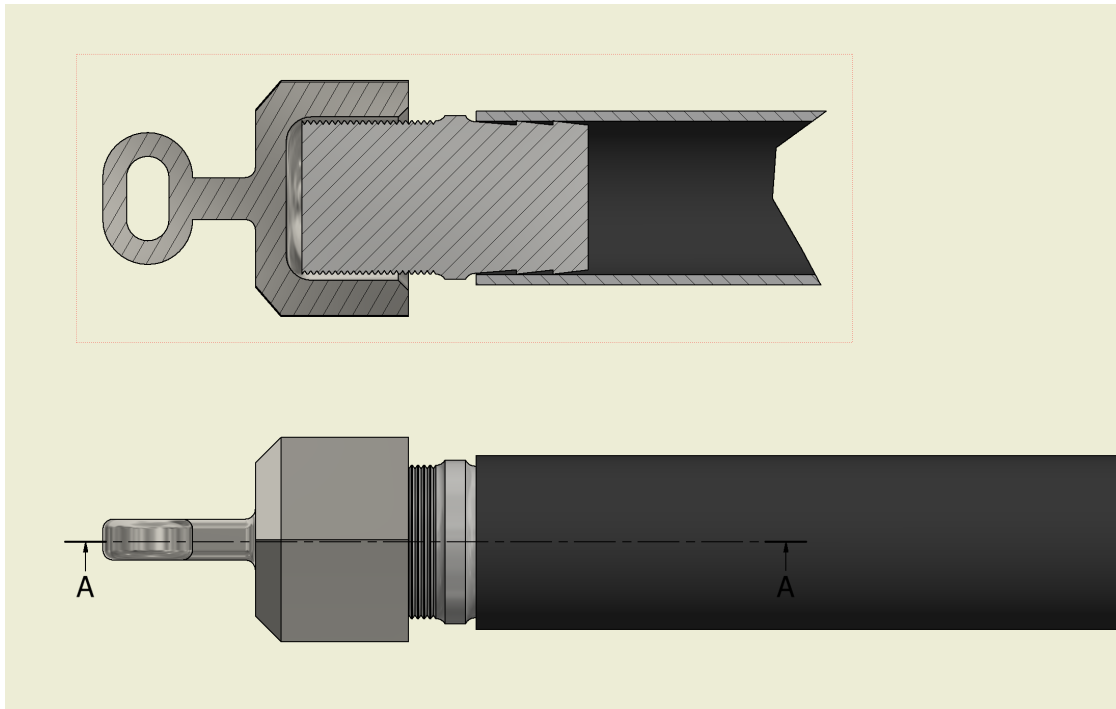


FIGURE 4.3: Concept fixings for the PAMs. (The outer mesh was not included but would be fixed between the threads and an air inlet should be added at one end)

4.4.2 Improving the Test Bench

Although solutions were improvised during testing, the sliding of the fixings was an issue as the test bench was designed for fixed lengths of 5", 8" and 11.5". A simple solution would be to connect the force gauge to a sliding element to adjust the length and pretension the PAMs accordingly.

Chapter 5

Conclusion

Spinal stability remains elusive in its complexity to be modeled and measured. However, in the context of the *robotic spine* project, McKibben style pneumatic artificial muscles provide a basis from which further insight can be developed. These prove to be useful physical analogs to the skeletal muscles having similar *force-displacement* and *force-pressure* properties despite differing in their *force-velocity* behaviour. Outlined in this study, was the striking linearity between force and pressure in the PAMs which correlate well with the behaviour found in the *tibialis anterior* of rabbits. By estimating the force in spinal muscles it was found that the PAMs provide a force of the same order of magnitude. That being said, certain simplifying assumptions while using the PAMs as a model for skeletal muscles should be kept in mind.

Indeed, the current artificial muscles being used in the *robotic spine* project do have limitations which essentially come down to their variability in performance, due to slipping at the fixings and non standardized assembly process. Changes were made which allowed for a greater range of force to be selected from and, in the case of the outer mesh modification, improved their reliability.

Other efforts to study these PAMs could be focused on further improvements in terms of reliability. Most notably, the fixings could be replaced by custom parts with rigid connections to prevent slipping and standardize assembly. Moreover, further testing could be done to study the effect that initial radius has on performance.

In closing, the PAMs used in the *robotic spine* project, while presenting certain limitations, proved to be a good starting point for a physical model of skeletal muscles. Despite their simplicity, they are a useful tool which allow for an alternative approach to studying spinal stability, contributing to the larger effort of understanding and treating disability caused by back pain.

Bibliography

- [1] D. Hoy et al. "The global burden of low back pain: estimates from the global burden of disease 2010 study". *Annals of Rheumatic Diseases* 73.6 (2014), pp. 968–74. DOI: [10.1136/annrheumdis-2013-204428](https://doi.org/10.1136/annrheumdis-2013-204428).
- [2] D.I. Rubin. "Epidemiology and risk factors for spine pain". *Neurologic Clinics* 25.2 (2007), pp. 353–71. DOI: [10.1016/j.nc1.2007.01.004](https://doi.org/10.1016/j.nc1.2007.01.004).
- [3] J. Hartvigsen et al. "What low back pain is and why we need to pay attention." *The Lancet* 391.10137 (2018), pp. 2356–2367. DOI: [10.1016/S0140-6736\(18\)30480-X](https://doi.org/10.1016/S0140-6736(18)30480-X).
- [4] R. Izzo et al. "Biomechanics of the spine - part I: spinal stability". *European Journal of Radiology* 82.2 (2013), pp. 118–126. DOI: [10.1016/j.ejrad.2012.07.024](https://doi.org/10.1016/j.ejrad.2012.07.024).
- [5] S.A. Go et al. "Design considerations of a fiber optic pressure sensor protective housing for intramuscular pressure measurements." *Annals of Biomedical Engineering* 45.3 (2017), pp. 739–46. DOI: [10.1007/s10439-016-1703-6](https://doi.org/10.1007/s10439-016-1703-6).
- [6] T.M. Winters et al. "Correlation between isometric force and intramuscular pressure in rabbit tibialis anterior muscle with an intact anterior compartment." *Muscle Nerve* 40.1 (2009), pp. 79–85. DOI: [10.1002/mus.21298](https://doi.org/10.1002/mus.21298).
- [7] J. Davis, K.R. Kaufman, and R.L. Lieber. "Correlation between active and passive isometric force and intramuscular pressure in the isolated rabbit tibialis anterior muscle". *Journal of Biomechanics* 36.4 (2003), pp. 505–12. URL: [10.1016/S0021-9290\(02\)00430-X](https://doi.org/10.1016/S0021-9290(02)00430-X).
- [8] A. White et al. "Biomechanical analysis of clinical stability in the cervical spine." *Clinical Orthopedics and Related Research* 109 (1975), pp. 85–96. URL: <https://www.ncbi.nlm.nih.gov/pubmed/1132209>.

- [9] K. Willis. "Presidential symposium on instability of the lumbar spine: introduction". *Spine* 10.3 (1985), p. 254. URL: https://journals.lww.com/spinejournal/Citation/1985/04000/Presidential_Symposium_on_Instability_of_the.12.aspx.
- [10] M. Panjabi. "Clinical spinal instability and low back pain." *J. Electromyography and Kinesiology* 13.4 (2003), pp. 371–79. DOI: [10.1016/S1050-6411\(03\)00044-0](https://doi.org/10.1016/S1050-6411(03)00044-0).
- [11] M. Panjabi. "The stabilizing system of the spine - part II: neutral zone and instability hypothesis". *Journal of Spinal Disorders* 5.4 (1992), pp. 390–97. URL: <https://www.ncbi.nlm.nih.gov/pubmed/1490035>.
- [12] M. Driscoll. "Biomechanics of musculoskeletal systems". *MECH 561 lectures at McGill University - Montreal, Canada* (2019).
- [13] W.K. Durfee and K.I Palmer. "Estimation of force-activation, force-length and force-velocity properties in isolated, electrically stimulated muscle". *IEEE Transactions on Biomedical Engineering* 41.3 (1994), pp. 205–16. DOI: [10.1109/10.284939](https://doi.org/10.1109/10.284939).
- [14] I. El Bojairami and M. Driscoll. "Correlating skeletal muscle output force and intramuscular pressure via a 3-dimensional finite element muscle model." *Journal of Biomechanical Engineering (Submitted)* (2019).
- [15] G. Belforte et al. "Soft pneumatic actuators for rehabilitation". *Actuators* 3.2 (2014), pp. 84–106. DOI: [10.3390/act3020084](https://doi.org/10.3390/act3020084).
- [16] G. Belforte et al. "Bellows textile muscle". *J. Textile Institute* 105.3 (2013), pp. 356–64. DOI: [10.1080/00405000.2013.840414](https://doi.org/10.1080/00405000.2013.840414).
- [17] B. Tondu. "Modelling of the McKibben artificial muscle: a review". *Intelligent Material Systems and Structures* 23.3 (2012), pp. 225–53. DOI: [10.1177/1045389X11435435](https://doi.org/10.1177/1045389X11435435).
- [18] FESTO. *Fluidic muscle DMSP/MAS*. Manufacturer's Manual. 2008. URL: https://www.festo.com/rep/en_corp/assets/pdf/info_501_en.pdf.
- [19] FESTO. *Airic's arm*. Manufacturer's Project Report. UNKNOWN. URL: https://www.festo.com/net/SupportPortal/Files/42058/Airics_arm_en.pdf.

- [20] B. Tondou et al. "A seven-degrees-of-freedom robot-arm driven by pneumatic artificial muscles for humanoid robots". *J. Robotics Research* 24.4 (2005), pp. 257–74. URL: <https://hal.archives-ouvertes.fr/hal-01292939/document>.
- [21] B. Verrelst et al. "The pneumatic biped "Lucy" actuated with pleated pneumatic artificial muscles". *Autonomous Robots* 18.2 (2005), pp. 201–13. DOI: [10.1007/s10514-005-0726-x](https://doi.org/10.1007/s10514-005-0726-x).
- [22] C. Chou and B. Hannaford. "Measurement and modelling of McKibben artificial muscles". *IEEE Transactions on Robotics and Automation* 12.1 (1996), pp. 90–102. DOI: [10.1109/70.481753](https://doi.org/10.1109/70.481753).
- [23] G.K. Klute, J.M. Czerniecki, and B. Hannaford. "McKibben artificial muscles: pneumatic actuators with biomechanical intelligence". *IEEE/ASME International Conference on Advanced Intelligent Mechatronics* (1999). DOI: [10.1109/AIM.1999.803170](https://doi.org/10.1109/AIM.1999.803170).
- [24] B. Tondou. "Modelling and control of the McKibben artificial muscle robot actuators". *IEEE Control Systems* 20.2 (2000), pp. 15–38. DOI: [10.1109/37.833638](https://doi.org/10.1109/37.833638).
- [25] M. Doumit, A. Fahim, and M. Munro. "Analytical modeling and experimental validation of the braided pneumatic muscle". *IEEE Transactions on Robotics* 25.6 (2009), pp. 1282–91. DOI: [10.1109/TR0.2009.2032959](https://doi.org/10.1109/TR0.2009.2032959).
- [26] R.L. Lieber and F.T. Blevins. "Skeletal muscle architecture of the rabbit hindlimb: functional implications of muscle design." *Journal of Morphology* 199 (1989), pp. 93–101.
- [27] L. Boissiere et al. "Lumbar spinal muscles and spinal canal study by MRI three-dimensional reconstruction in adult lumbar spinal stenosis". *Orthopaedics and Traumatology* 103.2 (2017), pp. 279–283. DOI: [10.1016/j.otsr.2016.10.025](https://doi.org/10.1016/j.otsr.2016.10.025).
- [28] W.H. Kim, S.H. Lee, and D.Y. Lee. "Changes in the cross-sectional area of multifidus and psoas in unilateral sciatica caused by lumbar disc herniation". *J. Korean Neurosurg. Soc.* 50.3 (2011), pp. 201–204. URL: [10.3340/jkns.2011.50.3.201](https://doi.org/10.3340/jkns.2011.50.3.201).

- [29] C. Dehner et al. "Intramuscular pressure, tissue oxygenation, and muscle fatigue of the multifidus during isometric extension in elite rowers with low back pain." *J. Sport Rehabil.* 18.4 (2009), pp. 572–81. URL: <https://www.ncbi.nlm.nih.gov/pubmed/20108857>.

Appendix A

Data

TABLE A.1: Data from testing the PAMS

Original 5"				Original 8"				Original 11.5"				Inner Tube Mod.				Outer Mesh Mod.			
Mean		Std. Dev.		Mean		Std. Dev.		Mean		Std. Dev.		Mean		Std. Dev.		Mean		Std. Dev.	
IN	OUT	IN	OUT	IN	OUT	IN	OUT	IN	OUT	IN	OUT	IN	OUT	IN	OUT	IN	OUT	IN	OUT
0	0	0.0	0.0	0	0	0.0	0.0	0	0	0.0	0.0	0	0	0.0	0.0	0	0	0.0	0.0
3	0	1.9	0.0	5	0	2.4	0.0	6	0	0.7	0.0	15	0	3.3	0.0	4	0	2.6	0.0
9	0	1.8	0.0	12	0	2.4	0.0	13	2	2.7	3.6	25	3	4.3	5.3	8	0	3.2	0.0
16	1	1.9	3.1	19	2	4.6	3.2	22	6	4.0	4.7	36	11	4.7	7.6	14	1	3.9	2.2
24	7	2.2	6.1	29	6	7.5	4.5	31	12	5.5	7.8	49	20	4.4	12.3	20	6	4.2	4.1
34	13	3.1	9.2	40	13	7.5	10.3	42	21	6.6	12.4	61	33	6.0	16.5	26	13	4.7	7.7
46	22	4.5	12.1	51	24	8.5	14.6	53	32	7.5	15.7	75	46	5.9	17.1	33	20	4.5	9.5
57	31	4.0	13.9	63	34	9.8	16.9	65	46	9.4	16.2	87	60	6.3	17.9	40	29	6.0	9.6
68	42	5.4	15.6	74	46	10.4	18.7	77	59	8.8	18.0	103	75	7.5	18.6	49	37	6.4	9.7
79	53	5.9	17.6	86	59	11.5	20.3	90	70	9.6	19.8	116	89	7.9	19.9	57	46	7.5	9.7
91	65	6.9	16.8	99	71	13.1	21.4	103	85	12.5	18.1	131	105	9.7	20.4	67	56	6.8	10.3
101	78	8.7	18.9	111	83	14.6	22.6	115	100	13.2	19.8	144	120	11.2	20.5	74	64	7.9	11.8
113	89	9.6	20.2	122	97	15.1	23.7	130	113	12.8	20.8	158	135	11.9	20.8	83	75	8.8	12.0
122	101	11.3	20.1	133	110	16.3	25.7	143	127	12.8	21.7	171	151	13.8	21.0	93	84	10.0	12.6
134	112	11.8	21.6	144	122	18.5	27.1	157	142	14.9	21.4	186	165	14.0	22.5	100	93	11.5	13.8
145	123	14.9	22.2	154	134	20.3	28.7	170	156	14.4	22.4	200	180	14.8	23.2	110	102	12.7	14.7
155	134	16.1	22.7	163	147	21.6	30.1	183	170	15.2	22.6	213	195	15.8	22.7	117	112	13.5	14.6
164	146	18.9	23.8	175	160	25.0	30.9	197	185	16.7	23.5	228	211	16.8	23.3	125	120	15.1	15.6
172	156	22.3	25.0	184	172	27.3	31.9	209	198	18.4	23.9	243	224	18.7	23.5	132	128	15.9	16.5
181	168	22.9	25.5	195	183	29.4	33.7	220	211	20.7	23.6	254	241	20.7	24.7	141	136	15.6	16.9
191	178	25.4	26.7	204	195	30.6	34.8	233	225	22.6	25.3	268	256	19.3	23.9	148	145	16.6	18.2
198	189	26.3	27.7	214	206	32.1	36.7	244	239	24.9	25.9	281	271	23.8	26.1	156	153	17.9	18.1
205	200	27.7	27.4	224	220	34.1	36.3	256	254	26.4	26.3	292	288	25.8	25.3	164	162	18.4	19.1

Appendix B

Bill of materials

TABLE B.1: Bill of materials used in the construction of the test bench.

Part Name	Quantity	McMaster #	Cost (CAD\$)	Comments
Wood Plank	1	N/A	3	-
Turnbuckle	1	3010T27	1.12	-
Carabiner	2	3885T11	1.68	-
Eyebolt	1	30455T63	8.31	Pack of 5
Pressure Gauge	1	3847K71	11.9	-
Force Gauge	1	N/A	49.95	https://tinyurl.com/yyj3vb5b
Air Pump	1	N/A	N/A	Pre owned
Tee Adapter	1	5779K227	8.18	-
Tubing	N/A	5635K62	N/A	From scraps

TABLE B.2: Bill of materials used to modify the original PAMs.

Part Name	Quantity	McMaster #	Cost (CAD\$)	Comments
Super-Soft Tubing	1	5234K81	14.6	10 ft.
Abraison Resistant Sleaving	1	9337K6	11.07	10 ft.
Original Polyester Sleaving	1	9284K4	4.89	10 ft.
Original Inner Tubing	N/A	5635K62	N/A	From scraps

Appendix C

Muscle force estimation

To estimate of the force in the spinal muscles, the *multifidus* was chosen as a point of comparison based on available data. Its cross sectional area (CSA) is approximately 6.8 cm^2 , and pressure during contraction, between 180 and 220 mmHg (3.5 to 4.3 psi) [28, 29]. The *tibialis anterior* on other hand has a volume of 3.4 cm^3 with a cross sectional area of 0.6 cm^2 [26].

The slope of the *tibialis anterior*'s force-pressure curve in Figure 4.2 was found to be 16.7 N/psi . Due to the linearity of the curve, the assumption was made that one could scale the force and pressure to estimate the force of another muscle. This would be based on the CSA of the muscle and scale the slope of the curve found for the *tibialis anterior*.

A scaling factor was found by dividing both CSAs:

$$SF = \frac{CSA_{multifidus}}{CSA_{tibialis}} = 11.5 \quad (\text{C.1})$$

By multiplying SF by the slope of the *tibialis anterior*, a theoretical slope for the *multifidus* can be estimated. Assuming an intercept with the origin, the force as

a function of pressure for the *multifidus* is the following:

$$F(P)_{multifidus} = 192P \quad (C.2)$$

Therefore the force at a median pressure of 3.9 psi is approximately **750 N**. This is of course a gross approximation but nevertheless gives an idea of the order of magnitude of the forces that could be produced by spinal muscles.